Number and orientation of fault sets in the field and in experiments

Atilla Aydin*
Department of Geology, Technical University of Istanbul, Istanbul, Turkey
Ze'ev Reches
Department of Applied Mathematics, Weizmann Institute of Science, Rehovot, Israel

ABSTRACT

Arrays of faults that can be grouped into multiple sets occur in the Entrada and Navajo Sandstones in southeastern Utah. The faults form a network that usually has a rhombohedral pattern both in map and cross-sectional views. Similar fault patterns were formed experimentally in cubic samples of sandstone, limestone, and granite deformed to failure with a polyaxial apparatus. The faulting theory of Anderson fails to explain both the number and the orientation of the faults observed in this study. However, the number and orientation of faults can be understood in terms of a theory of deformation of rock solely by slip along planes.

INTRODUCTION

Faulting is a process in which rocks fail along multiple surfaces or planes, which usually have several different orientations. Although faults are depicted on geologic maps as single lines, the structures depicted generally comprise many fault surfaces. Rocks deformed in the laboratory also fail along multiple surfaces. The fault surfaces both in the field and in laboratory samples are systematic and can be classified according to geometric relations. The simplest pattern is that of a single set of parallel or subparallel faults. A more complicated pattern composed of two sets of faults, often called conjugate sets, has been the subject of numerous studies. Anderson (1951) used the Coulomb theory to explain the formation and orientation of two sets of faults. Brace (1960) extended the Griffith theory for the same purpose. Odé (1960) made use of the slip-line theory of plasticity to account for patterns of two sets of faults.

Several investigators have reported that more than two sets of faults develop during a single period of deformation. These were observed in the field (Aydin, 1977; Reches, 1978; Mitra, 1979), in clay (Oertel, 1965), and in rock samples deformed in the laboratory (Z. Reches and J. Dieterich, in prep.). Oertel (1965) and Reches (1978) attempted to explain this phenomenon by analyzing slip on faults under a three-dimensional strain field.

We present here field and experimental results which show that faults generally occur in four sets.

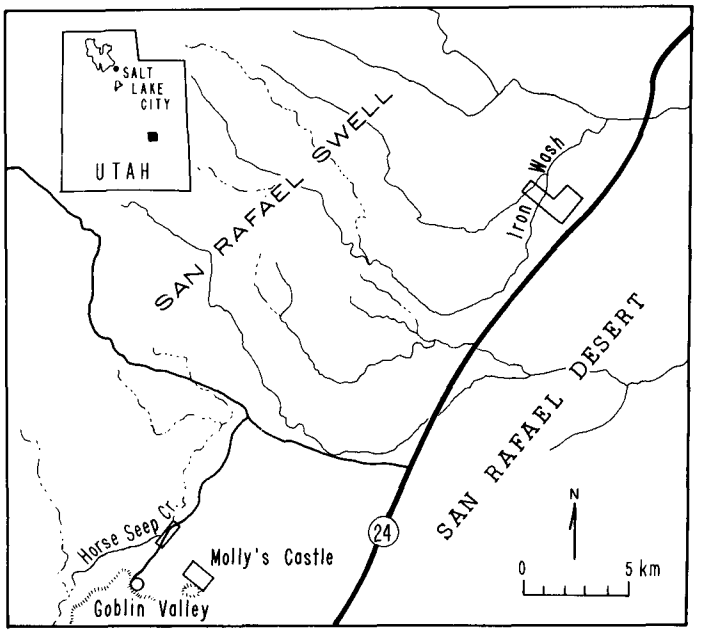

Figure 1. Map showing locations of study areas.

FIELD OBSERVATIONS

Multiple sets of faults occur at a wide range of scales in the field. Most of the geometrical features of such fault sets, however, can be readily recognized at the outcrop scale. We studied nearly normal faults in the Entrada and Navajo Sandstones in southeastern Utah (Fig. 1). Figure 2 shows the fault patterns in the Entrada Sandstone exposed at the Horse Seep Creek area. The map and the stereograms for five stations define three domains in terms of the patterns and the spatial distribution of the faults. The central domain includes stations II, III, and IV, and the other two include stations I and V. Figure 3a shows a plan view of the pattern of some of the faults at station II in the central domain. The linear features that form a network in the figure are the traces of numerous normal faults with offsets ranging from a few millimetres to a few centimetres. These faults divide the parent rock into rhombohedron-shaped blocks, characteristic of such multiple fault sets. The two faults that trend longitudinally in Figure 3a share the same strike, but they dip in opposite directions. The other faults are approximately aligned and are oriented obliquely (by about 20°) to the traces of the longitudinal faults. Most of the oblique faults dip to the right, but at least one of them (close to the scale bar) dips to the left. Thus, the faults shown in Figure 3a have four orientations. Stereographic projections of 29 fault planes measured at this station and statistical analysis of these data by follow-

*Present address: Department of Geosciences, Purdue University, West Lafayette, Indiana 47907.

ing Fisher (1953) confirm this observation (Fig. 2). Circles of 95% confidence, appearing in this projection as ellipses, have been drawn around the mean direction for each set, thereby separating four distinct fault sets. Similarly, stereographic projections and statistical analyses of fault-plane attitudes measured at stations III and IV show four fault sets (Fig. 2).

The pattern of faults at station V is shown in Figure 3b. In this illustration some faults trend longitudinally and others trend transversally. The angle between the trends is about 70°, which is larger than the corresponding angle in the central domain. Each trend represents a pair of fault arrays defined by two different dip directions. Geometrical features of faults at station I are similar to those of faults at station V. Four or perhaps five sets of faults are apparent at these two stations, as shown in the stereographic projections in Figure 2. Some of the fault sets at these two stations can be separated statistically; these are shown by 95% confidence circles drawn around the mean directions (Fig. 2). Statistical treatment of groups of data comprising three or fewer data points is inconclusive; therefore, circles of 95% confidence level for these groups have not been shown in Figure 2.

The relative ages of the multiple sets, based on crosscutting and offsetting relations of the faults, are also shown in Figure 2. Faults that are offset by other faults are termed "older" (O), as opposed to "younger" (Y). At some stations the longitudinal faults are older than the transversal faults; at other stations the reverse is true. This age relationship indicates that the multiple sets of faults in this outcrop formed during one stage of deformation—that is, they are essentially contemporaneous.

The cross-sectional views of the fault arrays are similar to the plan views described earlier. Figure 4a shows many small normal faults, which are distributed over a nearly vertical surface of the Entrada Sandstone in the Iron Wash area, San Rafael Desert, Utah. There are two apparent groups of traces of fault planes, one facing to the right and the other to the left in Figure 4a. These fault traces bound rhombohedral blocks of the parent rock. Figure 4b shows a sandstone block bordered by faults dipping in opposite

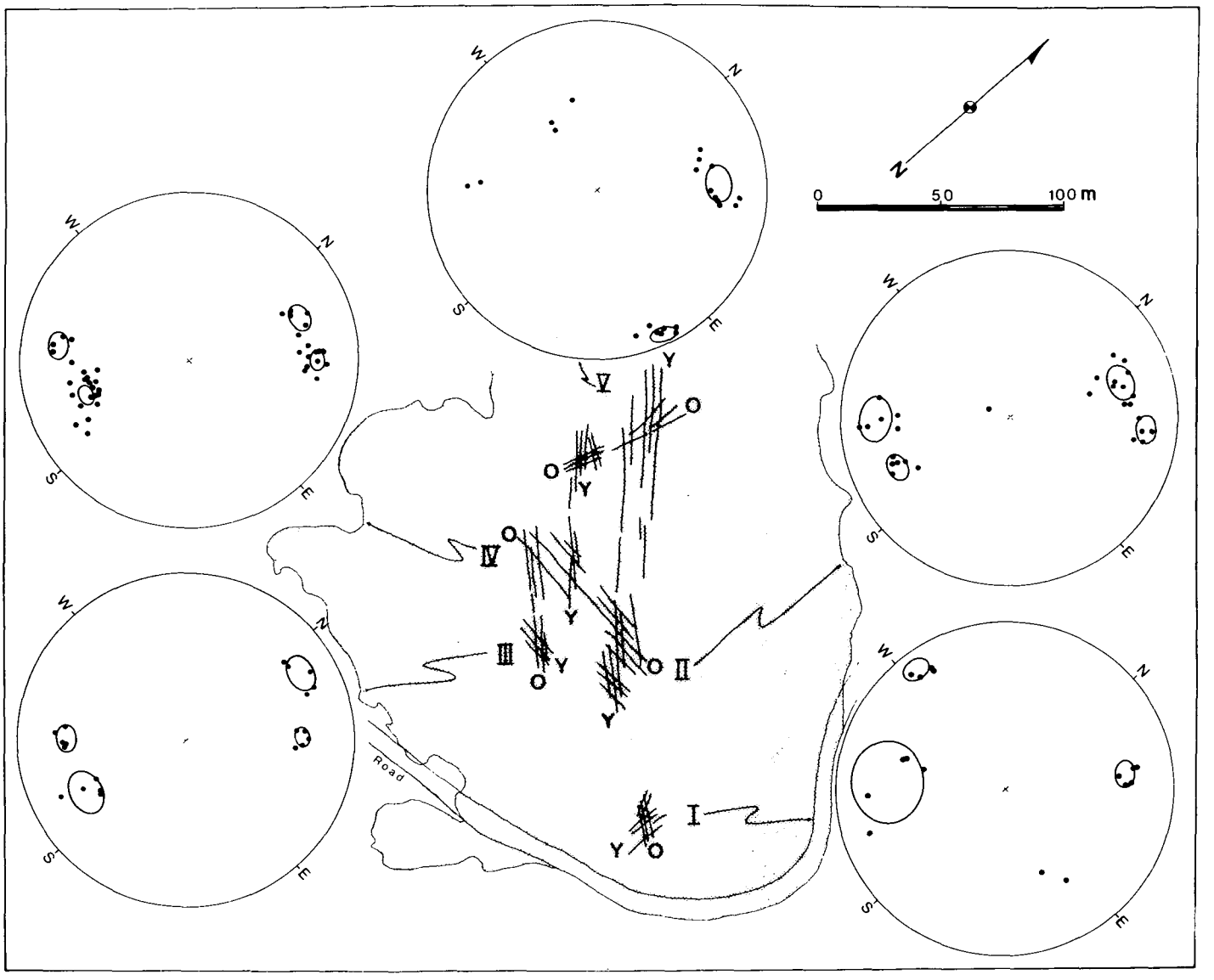

Figure 2. Map and stereographic projections of small faults in Horse Seep Creek area in San Rafael desert, Utah. Roman numerals indicate measurement stations. Y and O designate traces of younger and older sets, respectively. Stereographic plots are projections of poles of measured fault planes at a given station on lower-hemisphere, equal-area net. Ellipses are projections of circles of 95% confidence, drawn around mean directions for each set defined by four or more data points.

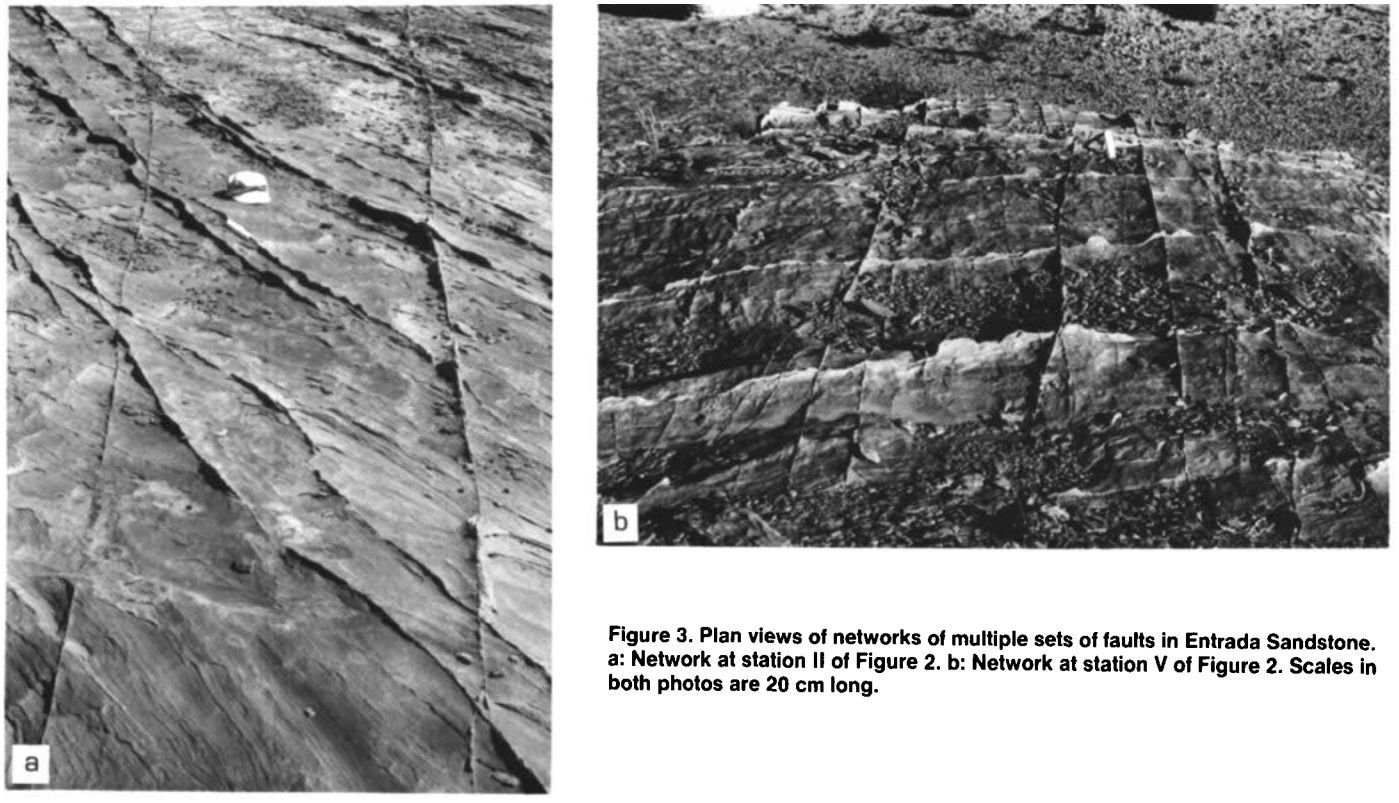

Figure 3. Plan views of networks of multiple sets of faults in Entrada Sandstone. a: Network at station II of Figure 2. b: Network at station V of Figure 2. Scales in both photos are 20 cm long.

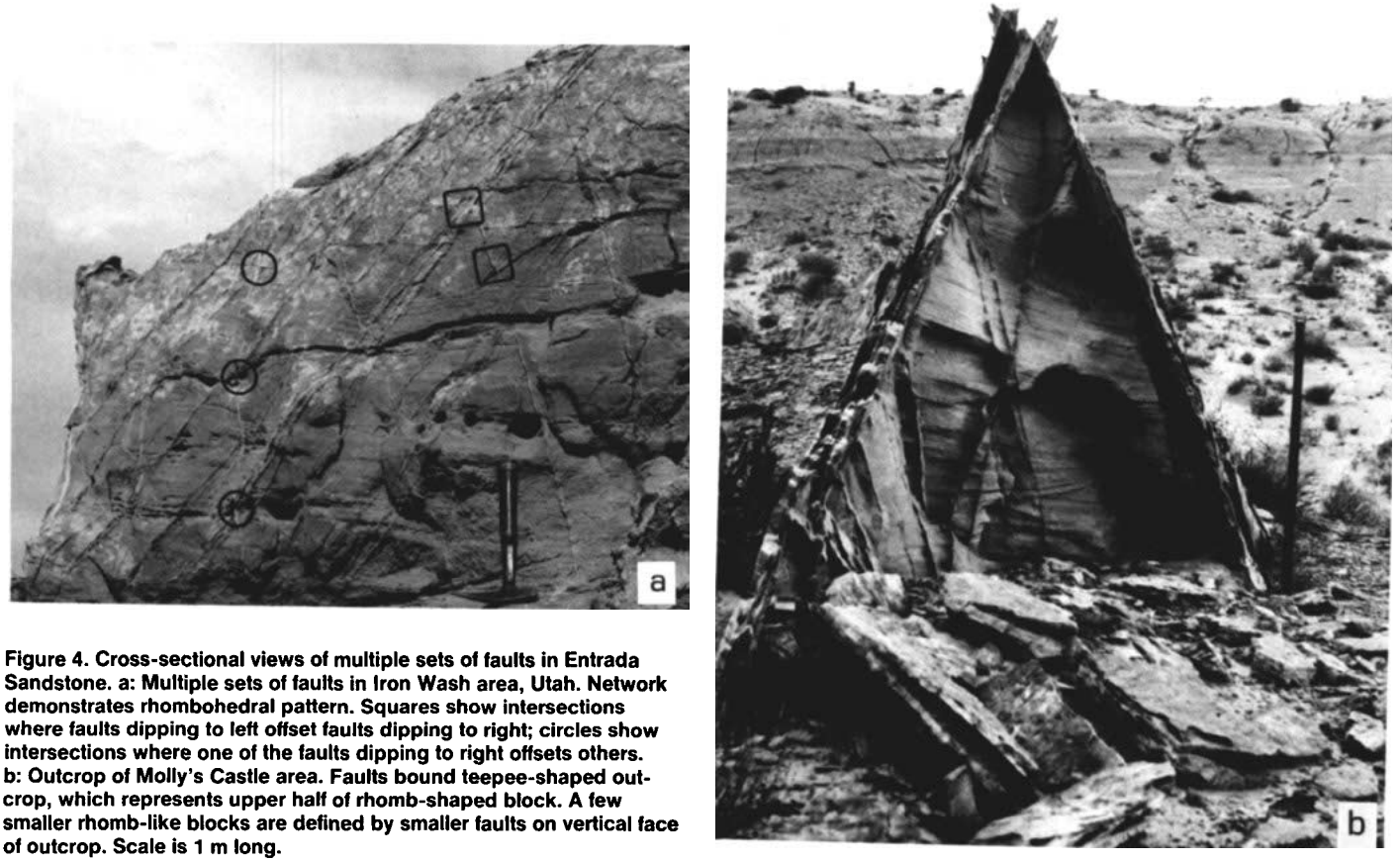

Figure 4. Cross-sectional views of multiple sets of faults in Entrada Sandstone. a: Multiple sets of faults in Iron Wash area, Utah. Network demonstrates rhombohedral pattern. Squares show intersections where faults dipping to left offset faults dipping to right; circles show intersections where one of the faults dipping to right offsets others. b: Outcrop of Molly's Castle area. Faults bound teepee-shaped outcrop, which represents upper half of rhomb-shaped block. A few smaller rhomb-like blocks are defined by smaller faults on vertical face of outcrop. Scale is 1 m long.

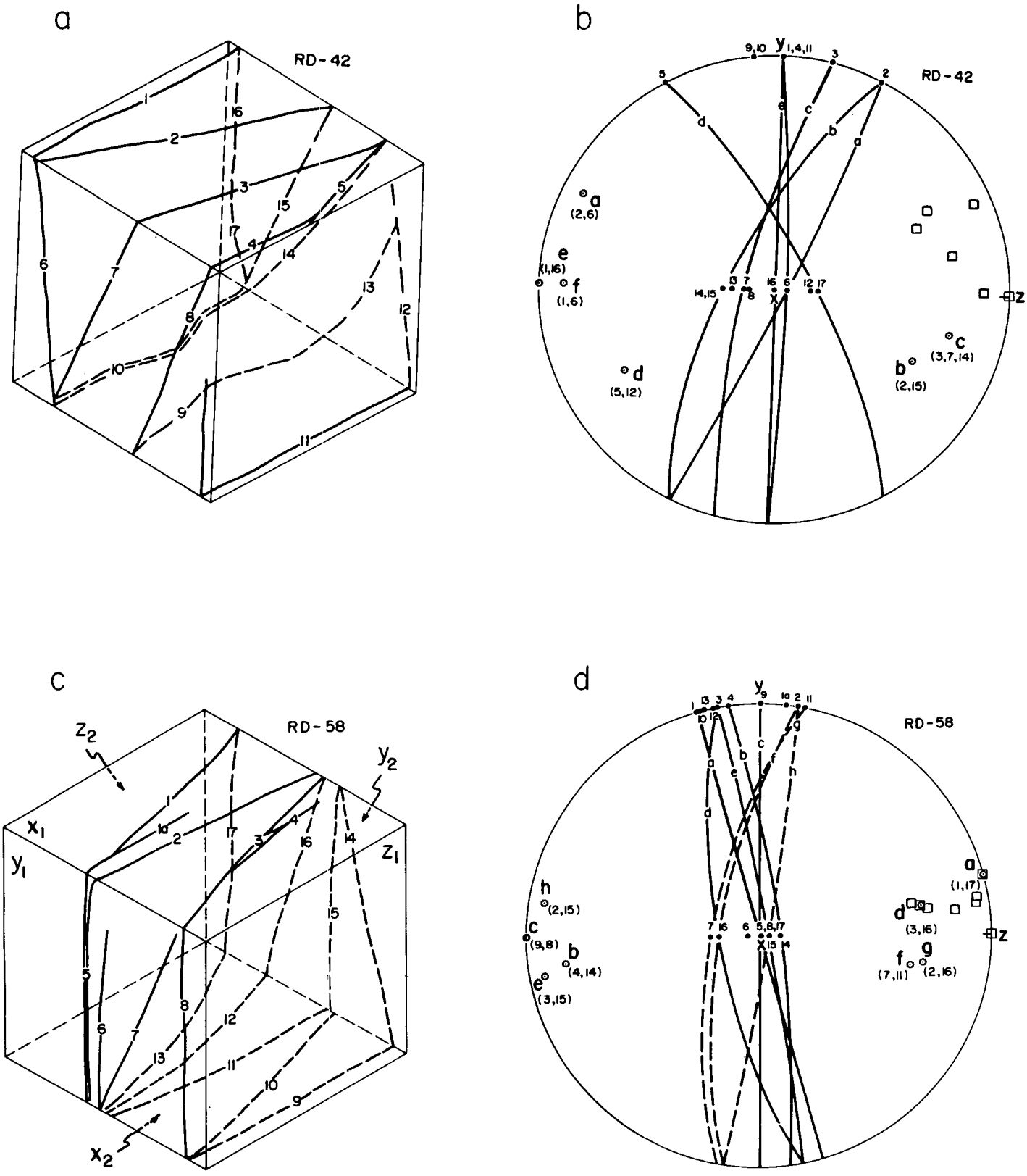

Figure 5. Determination of orientations of faults in two experiments, RD-42 of Berea Sandstone and RD-58 of Sierra White Granite. a and c: Block diagrams of faulted samples. Fault traces marked as solid lines on x_1, y_1, and z_1 faces and as dashed lines on x_2, y_2, and z_2 faces. b and d: Traces numbered in block diagrams are plotted on stereographic projections. Wulff net, lower hemisphere. Traces that belong to same fault surface are connected with great circle, and pole to this fault is marked and numbered. Numbers in brackets under pole symbols identify traces used to recognize this fault. Square indicates pole rotated according to orthorhombic symmetry.

directions to form a teepee-like structure. The face of the teepee is the upper half of a larger rhombohedral block. Within the face, smaller faults define smaller rhomb-like areas. It is difficult to determine the number of fault sets by examining cross-sectional views only. However, it is easier to observe the offsets at the intersections of the normal faults, where obviously younger faults offset the older ones. For example, in Figure 4a, faults dipping to the left commonly offset faults dipping to the right (squares). On the other hand, one of the faults dipping to the right offsets the faults dipping to the left (circles) indicating that at least the fault sets dipping in opposite directions formed approximately simultaneously.

Additional examples of the occurrence of more than two sets of faults of various dimensions were presented by Aydin (1977). Reches (1978) has reported four sets of faults with orthorhombic symmetry in sandstone in Grand Canyon, Arizona. Mitra (1979) observed four to seven sets of faults in granite and gneiss in the central Appalachians. The pattern of large-scale faults in the Basin and Range province (Donath, 1962) is very similar to the rhombohedral pattern of the small faults described above. Indeed, this pattern of faults is characteristic of the rift regions of Earth. For example, geologic maps of the Rhine Graben (Illies, 1977), the Rio Grande Rift (Yates and Thompson, 1959; Kelley, 1979), and the East African Rift (Walsch, 1966) illustrate rhombohedral patterns comprising four sets of normal faults in separate domains and perhaps even more sets on a regional scale.

EXPERIMENTAL RESULTS

Many failure tests have been made on rocks under uniaxial (σ_1, $\sigma_2 = \sigma_3 = 0$) or triaxial (σ_1, $\sigma_2 = \sigma_3$) conditions. Development of one or two sets of faults has been reported in these experiments (for example, Brace, 1964; Friedman and Logan, 1973). A few polyaxial experiments under more general stress conditions ($\sigma_1 > \sigma_2 > \sigma_3$) have been made on rock samples (Hojem and Cook, 1968; Mogi, 1971). However, the number of fault sets and their orientations were not reported for these polyaxial tests.

Reches and J. Dieterich (in prep.) performed a series of polyaxial experiments on cubic samples (22× 22× 22 mm) of Berea Sandstone, Sierra White Granite, and Candoro Limestone. The deformation apparatus used in the experiment has three mutually perpendicular hydraulic pistons, two of which, designated x and y, were servo-controlled by a computer. Displacements and stresses in the three axes were monitored continuously during all experiments. The use of a servo-control system significantly increased the stiffness of the apparatus and permitted constant strain rate during the entire experiment. The x, y, and z axes are the principal axes of the deformation. The strain rates in the x and y directions were kept constant during the experiment, whereas the strain rate in the z direction was determined by the response of the sample. The ratio of the strain rates, $k = \dot{e}_y/\dot{e}_x$, ranges from 4.0 to -0.4 in the experiments, where $k = 0$ indicates plane strain and $k \neq 0$ indicates three-dimensional strain.

The determination of the orientations of the faults in the 28 deformed samples is illustrated here by two examples, RD-42 of Berea Sandstone and RD-58 of Sierra White Granite (Fig. 5). The traces of faults and fractures observed on the faces of the cubic samples are shown on a block diagram on the left side of the figure. These traces are marked as solid dots on the projection on the right. By splitting the faulted samples or observing the intersection points of the edges of the samples, we are able to recognize which traces are associated with the same fault. For example, in experiment RD-58, trace 1 on the x_1 face, trace 17 on the y_2 face, and trace 13 on the x_2 face (Fig. 5c) are associated with one fault designated as a on the stereographic projection on the right (Fig. 5d). The other faults in the sample were determined by the same method. Typically, there are three to eight faults in each sample. By using the principal planes as symmetry planes, we divided these faults into two, three, or four sets. For example, we recognize three sets of experiment RD-42 (Fig. 5b) (set 1: faults a, e, f; set 2: faults b, c; set 3: fault d) and four sets of experiment RD-58 (Fig. 5d). These sets are arranged in an orthorhombic symmetry with respect to the x, y, and z axes (right side, Fig. 5). The orientations of faults in all samples were determined this way.

We rotated the poles to the faults according to the orthorhombic rule into one quarter of the stereonet (rotated poles are shown as open squares in the upper right quarter of the stereonets of Fig. 5). We consider the *average fault*, calculated after rotation of all poles into one quarter, as the representative of all faults in the experiment. The standard deviation (Fisher, 1953) of the average fault in all samples ranges from 2.6° to 13.1°, with 6.1° as the mean value. The circle of 95% confidence level of the average fault in all samples ranges from 1.6° to 12.6°, with 5.7° as the mean value. When the average fault occurs on one of the principal planes, xy, xz, or yz, it represents two sets in a conjugate pattern,

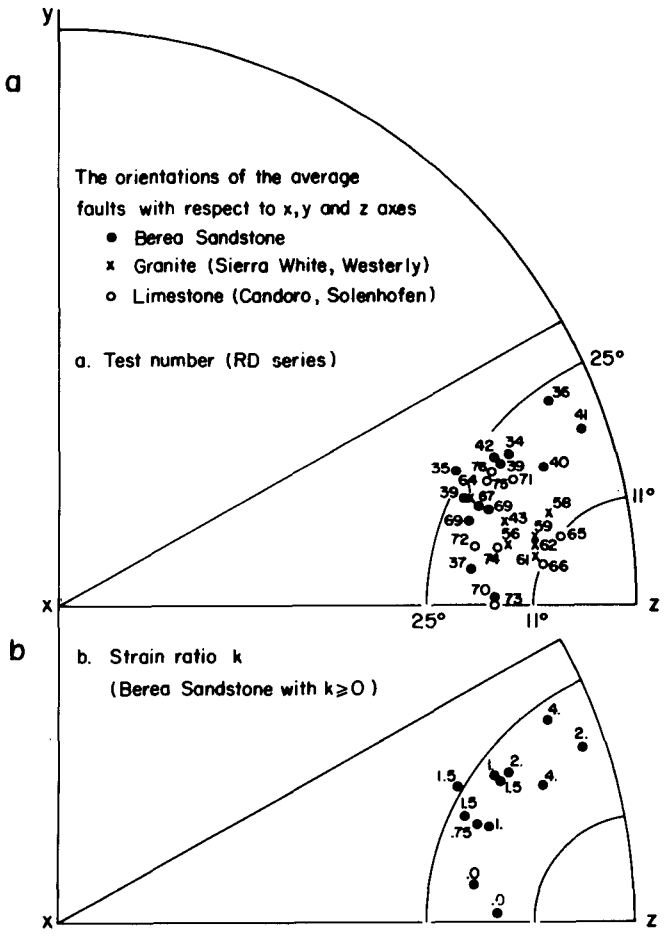

Figure 6. a: Average faults of all samples plotted in 30° section of stereonet projection (see Fig. 5). Wulff net, lower hemisphere. Two small circles in figure have radii of 11° and 25° around z axis. b: Average faults of Berea Sandstone samples.

and when this fault occurs away from the principal planes, it represents three or four sets of faults.

The poles to the average faults of all 28 experiments are plotted in Figure 6a. The poles to the average faults in the experiments with Berea Sandstone are shown separately in Figure 6b. The orientations of the average faults in these sandstone samples display a clearer trend than the orientations of the average faults of the other rock types.

One can recognize the following features in Figure 6: The poles to all average faults are distributed between the xz plane and the yz plane, oriented from 11° to 25° with respect to the z axis (Fig. 6a). The orientations of faults in the twelve samples of Berea Sandstone vary systematically with the experimental strain ratio $k = e_y/e_x$ (Fig. 6b); the faults of samples with large strain ratio, $k \geq 2$, fall close to the yz plane, the faults of samples with intermediate strain ratio, $1.5 \geq k \geq 0.75$, fall between the xz and yz planes, and the faults of the two samples with $k = 0$ fall closer to the xz plane (Fig. 6b). The circle of 95% confidence level for these samples ranges from 2.1° to 12.6°, with 6.8° as the mean value. These features indicate that the fault pattern in samples that underwent three-dimensional deformation, $k \neq 0$ (where $k = \dot{e}_y/\dot{e}_x$), tend to be *orthorhombic,* with *three* or *four* fault sets. On the other hand, the fault pattern in samples that underwent plane strain, $k = 0$ (for example, experiments RD-37, 62, 70, 73; Fig. 6a), tends to be a *conjugate* set with *two* fault sets. Furthermore, the sandstone samples (Fig. 6b) show systematic variations of the orientation of the average fault with the strain ratio.

DISCUSSION AND CONCLUSIONS

The rhombohedral patterns of normal faults described here are quite common in nature. Similar fault patterns have been reported by Woodring and others (1940), Yates and Thompson (1959), Walsch (1966), Donath (1962), Illies (1977), and Kelley (1979). These observations of the number of fault sets and their orientation are different from those predicted by the faulting theories developed by Anderson (1951), based on the Coulomb criterion; by Brace (1960), based on the Griffith criterion; and by Odé (1960), based on the slipline theory of plasticity. The Coulomb and Griffith criteria predict two sets of failure planes, and the slipline theory predicts two surfaces of discontinuity in velocity which presumably are analogous to two sets of faults. A few theoretical analyses, however, predict more than two sets of faults. Oertel (1965) suggested that interference among fault sets can explain four sets of faults that he produced in clay cake experiments. Reches (1978) analyzed slip along multiple faults and showed that, if the applied external strain is accommodated solely by slip along faults, four sets of faults are sufficient and necessary to accommodate three-dimensional strain. It appears that Anderson's (1951) theory of faulting deals with plane-strain conditions as far as the strain associated with faulting is concerned. Although plane-strain conditions may exist in nature, three-dimensional strain conditions should be expected for general cases.

In summary, we have shown that more than two sets of faults develop more or less simultaneously both in the field and in laboratory experiments. These faults in outcrop and in laboratory samples have distinct patterns, with orthorhombic symmetry. Evidently, faulting in a three-dimensional strain field with orthorhombic symmetry requires four sets of faults to accommodate strains in all principal directions.

REFERENCES CITED

Anderson, E. M., 1951, The dynamics of faulting: London, Oliver and Boyd, 183 p.

Aydin, A., 1977, Faulting in sandstone [Ph.D. thesis]: Stanford, California, Stanford University, 246 p.

Brace, W. F., 1960, An extension of the Griffith theory of fracture to rocks: Journal of Geophysical Research, v. 65, p. 3466–3480.

——1964, Brittle fracture of rocks, *in* Judd, W. R., ed., State of stress in earth's crust: New York, Elsevier, p. 110–174.

Donath, F. A., 1962, Analysis of Basin-Range structure, south-central Oregon: Geological Society of America Bulletin, v. 73, p. 1–16.

Fisher, R. A., 1953, Dispersion on a sphere: Royal Society of London Proceedings, ser. A, v. 217, p. 295–305.

Friedman, M., and Logan, J. M., 1973, Lüders' bands in experimentally deformed sandstone and limestone: Geological Society of America Bulletin, v. 84, p. 1465–1476.

Hojem, J.P.M., and Cook, N.G.W., 1968, The design and construction of a triaxial and polyaxial cell for testing rock specimens: South African Mechanical Engineering, v. 18, p. 57–61.

Illies, J. H., 1977, Ancient and recent rifting in the Rhinegraben, *in* Frost, R.T.C., and Dikkers, A. J., eds., Fault tectonics in N.W. Europe: Geologie en Mijnbouw, v. 56, p. 329–350.

Kelley, V. C., 1979, Tectonics, middle Rio Grande Rift, New Mexico, *in* Riecker, R. E., ed., Rio Grande Rift: Tectonics and magmatism: Washington, D. C., American Geophysical Union, p. 57–70.

Mitra, G., 1979, Ductile deformation zones in Blue Ridge basement rocks and estimation of finite strain: Geological Society of America Bulletin, Part I, v. 90, p. 935–951.

Mogi, K., 1971, Fracture and flow of rocks under high triaxial compression: Journal of Geophysical Research, v. 76, p. 1255–1269.

Odé, H., 1960, Faulting as a velocity discontinuity in plastic deformation, *in* Griggs, D., and Handin, J., eds., Rock deformation: Geological Society of America Memoir 79, p. 293–321.

Oertel, G., 1965, The mechanism of faulting in clay experiments: Tectonophysics, v. 2, p. 343–393.

Reches, Z., 1978, Analysis of faulting in three-dimensional strain field: Tectonophysics, v. 47, p. 109–129.

Walsch, J., 1966, Geologic map of the Eldawa Ravine–Kabarnet area, Kenya: Kenya Ministry of National Resources and Wildlife, Mines and Geological Department, scale 1:125,000.

Woodring, W. P., Steward, R., and Richards, R. W., 1940, Geology of the Kettlemen Hills oil field, California: U.S. Geological Survey Professional Paper 195, 169 p.

Yates, R. G., and Thompson, G. A., 1959, Geology and quicksilver deposits of the Terlingua district, Texas: U.S. Geological Survey Professional Paper 312, 114 p.

ACKNOWLEDGMENTS

Reviewed by G. Oertel, D. D. Pollard, and A. M. Johnson. Aydin was supported by the Weizmann Institute of Science during his stay at the Department of Applied Mathematics as a visiting scientist. The experiments reported in this study were carried out in cooperation with J. Dieterich, U.S. Geological Survey.

MANUSCRIPT RECEIVED MAY 20, 1981
REVISED MANUSCRIPT RECEIVED AUGUST 31, 1981
MANUSCRIPT ACCEPTED NOVEMBER 19, 1981